STRESSES WITHIN ROLLS WOUND IN THE PRESENCE OF A NIP ROLLER

J.K. Good, Z. Wu and M.W.R. Fikes

School of Mechanical and Aerospace Engineering

Oklahoma State University

Stillwater, OK USA

ABSTRACT

Models which can be used to calculate the internal stresses within wound rolls of web material have all been confined to the center winding technique to date. In this publication a new boundary condition is presented which will allow existing models to calculate the internal stresses within a wound roll which has been center wound with an undriven nip roller impinged upon the outside of the roll. Experimental verification of the new boundary condition is presented. The mechanism by which a nip roller can increase the wound in tension in the outer layer of the wound roll is presented.

NOMENCLATURE

b=Hertzian half contact width, cm
E=Young's modulus, Pa
E_c=core stiffness, Pa
E_r=nonlinear radial roll modulus, Pa
E_θ=circumferential roll modulus, Pa
h=web thickness or caliper, cm
Li=distance between clamped support and the nip prior to rolling, cm
NRD=nip rolling distance, cm
r=radial wound roll coordinate, cm
s=radial location of outermost layer in roll, cm
T_w=tensile stress in outer layer of roll, Pa
u=radial deformation of wound roll normalized by dividing by outer core radius
x=machine direction coordinate, cm
ε_x=machine direction strain
ε_{web}=nip induced strain

σ_r=radial stress in wound roll, Pa
σ_θ=circumferential stress in wound roll, Pa
σ_x=machine direction stress, Pa
σ_y=stress normal to web plane, Pa
σ_z=cross machine direction stress, Pa
μ=coefficient of friction
ν=Poisson's ratio

INTRODUCTION

Web handling is a manufacturing process which pervades almost every manufacturing industry in one way or another. A web is a continuous, flexible strip of material such as paper, plastic film, metal foil, textiles, and non-woven materials which are stored at least on an intermediate basis in wound rolls to accommodate high speed, automated manufacturing operations. Web handling is the science involving the mechanics and dynamics of transporting webs from unwind stations, through process machinery, to rewind stations.

Winding is an integral operation in almost every web handling process. During the course of a web becoming a final converted product it may be unwound and rewound several times depending upon the number of web processes which must be performed. Winding exerts stresses and curvatures upon webs which often can degrade the web quality but the wound roll form is the most efficient and opportune storage format for high speed automated manufacturing processes. It is desirable to wind just enough stress into a wound roll that a stable package is wound which has as few defects as possible which can result from too little or too much stress being wound into the roll.

Much of the winding which is currently performed is accomplished via a technique which is known as center winding with an undriven nip roll, refer to Figure 1. This technique requires that the winding torque be provided to the center(called the core) of the winding roll. An undriven nip roll follows the outside radius of the winding roll with a dual purpose. One purpose is to help exude wound-in air from the wound roll which could lead to an unstable, loosely wound roll package which is apt to sustain web defects during web storage or transport. The second purpose is to provide an increased tension in the web, above the web line tension, for the web winding process. This increased tension is due to a nip mechanics mechanism which heretofore has only been understood empirically. This publication is a presentation of results of analytical and experimental investigations which provide the first basic understanding of the nip induced tension mechanism. Some reference will be made to a machine direction. The machine direction in a web line is the direction in which the web travels through the web line.

There are several wound roll stress models in existence which differ mainly in the manner in which the web material properties are allowed to vary. All of these models apply only to the center winding technique without a nip roll. This publication will show that with the basic understanding of the nip induced tension mechanism that new boundary conditions can be developed for use with the existing wound roll models to model center winding with an undriven nip roll. Experimental results have been included to confirm that the new modeling technique is valid.

DISCUSSION

An empirical investigation of the effect of a rolling nip upon paper stacks resulted in a landmark publication by Pfeiffer[1]. In this publication, the first quantitative data was presented which showed the effects of nip load, nip diameter, and the number of sheets in the stack upon the nip induced tensions in the stack sheets. Pfeiffer noted in his tests that the sheets nearest the nip would displace in the direction of the moving nip while some of the sheets near the bottom of the stack would travel in the opposite direction. Using photomicrographs taken from the side of the nip/stack interface, he determined that the instant center of rotation did not lie at the nip/stack interface and in fact was located beneath the interface in the stack. Sheets above the instant center would travel in the direction of the rolling nip, sheets below would travel in the opposite direction.

Engineers and scientists have long been intrigued with the mechanism of rolling friction. In a classical paper Reynolds[2] proposed a theory for rolling friction in which he attributed the rolling resistance to causes essentially the same as those responsible for ordinary sliding friction. Reynolds observed that when a metal cylinder rolls over a flat rubber surface that the cylinder moves forward, in each revolution, a distance less than the circumference of the cylinder. From his earlier work regarding the slip of leather belts over cylindrical pulleys Reynolds[3] concluded that there was a similar kind of slipping between the roller and the rubber surface. Although Reynolds' conclusions were later discounted by Tomlinson[4] it is interesting that these experiments were very similar in setup to Pfeiffer's although certainly the goals of the experiments were dissimilar. Tabor[5] performed similar experiments which proved that there was an extension of the flat rubber prior to the inlet of the nip contact. Furthermore he discerned that there was no notable slip between the rubber and a steel nip during the period of contact. Tabor concluded that the mechanism of rolling friction and the associated energy loss was elastic hysteresis within the rubber.

The case of a nip rolling upon a web stack is fundamentally different from the case in which a nip is rolled across a relatively thick, homogenous solid such as rubber. Although slippage may not occur in the nip roll/web interface as described by Tabor, slippage can and does occur at the web sheet interfaces within the stack as will be shown. If this interlayer slippage can be determined as a function of nip load, nip diameter, and the available traction between web layers then the nip induced tension can be determined.

An investigation was launched which began with a simple experiment. The purpose of this experiment and associated analyses was to determine if elastic hysteresis needed to be present within the material over which the nip was rolled for the nip induced tension to occur.

EXPERIMENTAL PROCEDURE

An experiment was designed in which the effects of elastic hysteresis would be minimal. Both Tabor and Pfeiffer had employed rubber in at least portions of their experiments. Of course the temptation to use rubber is high as Young's modulus is so low that the deformations are high, to the extent that they are visible. There is also a large amount of inherent hysteresis within rubber materials. Thus an engineering material, aluminum, was selected which would

have low hysteresis but relatively high Young's modulus as the material which was to be rolled beneath the nip. Since the deformations would be small a precise means of determining the elongation and nip induced tensions would have to be incorporated.

The experimental apparatus is shown in Figure 2. An aluminum strip of a UNS A92024-T3(E= 72 GPa, ν=0.33) material, 3.81 cm wide and 0.0254 cm thick, is rigidly clamped at one end of the test table. A dead weight was applied to the opposite end of the aluminum strip whose primary purpose was to keep the strip aligned upon the test table although various weights could be applied to simulate the effect of varying the incoming web tension on the nip induced tension. A dead weight of 22.24 N was used in all experiments which provided a pre-tension of 2.30 MPa in the strip prior to nip rolling. Aluminum nip rolls of 5.08, 10.16, 15.24, and 20.32 cm diameters were rolled across the strip at nip loads of 3.5, 7, 10.5, 14, and 17.5 N/cm(load per unit width of nip contact). The combination of a nip diameter of 5.08 cm and a nip load of 17.5 N/cm exerted the maximum Hertzian contact stress of 28.8 MPa. Since the compressive yield strength for the aluminum is 275.6 MPa, the stresses exerted upon the aluminum strip during all experiments were definitely within the elastic range. The nip induced tension in the strip was sensed via strain gages that were oriented within a Wheatstone bridge to cancel any strains due to bending that might occur. The strain gage bridge was connected to a strain indicator. The analog output of the strain indicator was read by a data acquisition board which was resident in an IBM PC compatible computer, thus allowing the strain from which the nip induced tension could be inferred to be recorded. Each test for a given nip diameter and load was repeated five times and averaged to insure confidence in the data.

EXPERIMENTAL RESULTS

Since the stress in the strip after rolling is nominally uniform the uniaxial form of Hooke's Law($\sigma = E\varepsilon$) was applied to convert uniaxial strains to stresses. Figures 3 and 4 show the nip induced stresses overlaid upon the uniform pre-tensile stress discussed in the procedure for a 5.08 and 10.16 cm diameter nips, respectively. Data of similar form was recorded for 15.24, and 20.32 cm diameter nips as well. If a general form was given to all the data presented a relation such as:

$$\sigma_x = C_1\left[1 - e^{-C_2 x}\right] + C_3 \qquad \{1\}$$

would fit each and every curve well. In this relationship σ_x represents the total machine direction stress, C_1 represents the saturation value of the nip induced stress, C_2 represents the growth rate of the nip induced stress, and C_3 represents whatever pretension might have existed within the strip prior to the nip rolling.

In Figure 5 the saturation values of the total stress is shown versus nip load for various diameter nips. For each nip diameter, the saturated value of the total stress appears to be lineally dependent upon nip loading. For a differential tension to be sustained beneath the nip requires that a frictional force exists between the bottom of the aluminum strip and the steel test table which would be dependent upon the local sliding friction coefficient and the normal force or nip loading. Note that in Figure 5 a theoretical plot of the saturated value of the total stress has been included which depicts the experimental data quite well for its simplicity. These values were obtained by measuring the coefficient of friction via a test

defined by ASTM[1], multiplying the coefficient times the nip loading, dividing by the strip thickness, and adding the result to the pretension. Thus the explanation for the saturation in each of the curves in Figures 3 and 4 is that the nip induced tension has exceeded the product of the coefficient of sliding friction and the nip loading.

Although an explanation of why the nip induced tension reaches a saturation value has been given, no explanation has been given as to what the mechanism is which causes the nip induced tensions to occur prior to saturation. Finite element analyses will be employed to attempt to discern the mechanism.

FINITE ELEMENT ANALYSIS

The nip and the strip over which it is rolling might be modeled approximately as a Hertzian contact problem which was first described by Hertz [6] and rigorously studied by Radzimovsky [7]. This would indeed be an approximation as the bodies in contact are assumed to be large in comparison to the dimensions of the compressed area. The half width dimension of contact will commonly approach the web thickness and slippage is possible at the lower surface of the web.

A model concept was formulated and is shown in Figure 6 in which a moving, Hertzian parabolic pressure distribution would move across the upper surface of the web through time. The lower web boundary would be fully restrained vertically but only partially restrained horizontally to accommodate friction.

Since the width of the tested strip was quite large compared to the thickness (3.81 cm. vs 0.0254 cm.) the strip was assumed to conform to plane strain conditions. The web was therefore modelled as two dimensional plane strain elements on COSMOS^{TM}[2], a nonlinear finite element code. Nonlinear gap elements were placed upon the lower boundary to accommodate the slippage which must occur for a nip induced tension to result. The model definition, refer to Figure 6, portrayed the test apparatus described in the experimental procedure and consisted of 600 plane strain elements(0.00127 cm. x 0.00127 cm.) representing the web beneath the nip, 21 spring elements which represent the axial stiffness of the web between the nip and the clamped support(a distance of 37.29 cm), and 30 gap elements to accommodate the slippage below the web beneath the nip. In successive time steps, the Hertzian pressure profile shown in Figure 6 was moved to the right one element width.

RESULTS OF FINITE ELEMENT ANALYSIS

A 5.08 cm diameter aluminum nip with a 17.5 N/cm nip loading was chosen as one of several case studies. For this case the Hertzian half width of contact b is 0.00386 cm. and the maximum classical Hertzian contact pressure is 28814 kPa. In perusing the results the most interesting feature was that an elongating machine direction (x direction) strain exists on the lower surface of the web strip. A plot of the elongating strain on the bottom surface of the web beneath the nip location

[1] "Standard Test Method for Static and Kinetic Coefficients of Friction." ASTM, Vol. 08.02, pp. 133-137, 1989.

[2] COSMOS^{TM}/M, Structural Research and Analysis Corporation, 1661 Lincoln Boulevard, Suite 100, Santa Monica, CA, 90404.

is shown in Figure 7 at the eighth time step. At the following time step the strain plot would be nearly identical except that the peak strain would have moved one nodal location to the right of the previous peak value location. Note as well that the strain distribution is not symmetric about the peak value location which shows that an increase in the elongating strain exists across the nip due to the combination of the moving Hertzian pressure profile moving to the right over the upper surface of the web strip and the frictional forces on the lower surface. The maximum value of the elongating strain in Figure 7 is 4.92 μS. Thus as the nip passes over the web strip every point on the lower surface witnesses the elongating strain distribution shown in Figure 7 and the extension of the web strip due to the nip rolling over one finite element will be the integral of the strain, which is equivalent to the area under the curve in Figure 7. The area under the curve, using trapezoidal rule integration, is found to be $8.665*10^{-8}$ cm which is the deformation contribution from the nip rolling over an element which is .00127 cm in length. The deformation of the web due to the nip roll moving 1 cm will be $8.665*10^{-8}$ cm *(1cm/0.00127cm) or $6.823*10^{-5}$ cm of displacement for every 1 cm of rolling distance. The strain in the web strip can be calculated using the following algorithm:

$$\varepsilon_{web} = \frac{6.823x10^{-5} \text{ x N.R.D.}}{L_i + \text{N.R.D.}} \qquad \{2\}$$

Note that equation {2} is nonlinear with respect to the nip rolling displacement and is of the same form as equation {1}. For large nip rolling displacements equation {2} would yield that the web strain would approach a constant, however, experiments have shown that although a constant value is appropriate that the constant is dependent only upon the nip loading and the coefficient of friction as previously discussed and not the higher strain level which would predicted by equation {2}. The nip induced stress can be predicted using equation {2} for cases in which the saturated value of nip induced tension has not been achieved. The nip induced stress is calculated by multiplying the web strain by Young's modulus as the stress state in the web is unidirectional after passage of the nip. In Figure 8 the data from Figure 3 is presented again but note that only the first inch of rolling distance is now shown. The agreement between the experimental data and the finite element analysis is excellent. The comparison is made only over the first few centimeters of rolling distance as the slope of a curve through the experimental data begins to decrease due to slippage beginning to occur beneath the nip as the nip rolling distance increases as seen in Figure 3. In the finite element modeling the coefficient of traction between the aluminum web strip and the steel test table had to be selected. Early runs implemented coefficients of 0.085, which was the sliding coefficient of friction determined by tests in the laboratory. These early runs yielded nip induced tension rates an order of magnitude higher than that reported and it became evident that an entirely different regime of friction existed during the presaturated stage of nip induced tension than the sliding friction which was evident in the saturated stage as was discussed in the experimental results. During the presaturated stage the elongating strains on the lower surface are trapped by a high local contact pressure between the lower surface of the web strip and the test table. In this friction regime as the lower surface extends over the test table surface it requires that surface asperities on the web strip surface and the test table surface to become dislodged requiring plastic deformation. Friction coefficients in the range of 1 to 2 have been

reported for such cases by Bayer et al. [8]. Experimentation with the finite element model indicated that the elongating strain beneath the nip asymptotically approaches a minimum at coefficients near 2, a coefficient of 20 will not appreciably change the results. The coefficient of 2 was selected for reporting results since coefficients of friction higher than 2 have never been documented.

Another point of interest are the stresses which exist on a centerline beneath the point of contact between the nip roll and the web strip. The classical Hertzian contact stresses and the stresses computed by finite element analysis are shown in Figure 9. After noting the similarity in the forms a plot of the machine direction strain was constructed for both the Hertzian and finite element stresses as shown in Figure 10. Note that even though the classical Hertzian contact stresses are always compressive that throughout much of the depth of the strip that they result in a elongating machine direction strain. This is the heart of the nip induced tension mechanism. The three dimensional stress-strain relationship for the machine direction strain is:

$$\varepsilon_x = \frac{1}{E}[\sigma_x - \nu\,(\,\sigma_y + \sigma_z\,)] \qquad \{3\}$$

for isotropic materials. Given that all three Hertzian contact stresses are negative, compressive stresses, it is apparent that whenever the sum of the absolute values of σ_y and σ_z multiplied by Poisson's ratio is greater than σ_x that a positive machine direction strain, causing an elongation, will exist. This elongating strain distribution will proceed in the direction of rolling with material extending out in front of the nip and contracting behind the nip. If the material behind the nip is initially clamped the contraction is restrained and an increase in web strip tension between the nip and clamp will occur. This concept is shown in schematic form in Figures 11a and 11b. Even though the Hertzian stresses can be implemented in describing the phenomena, finite element analyses are still required if it is desired to accurately determine what the rate of nip induced tension will be with respect to the nip rolling distance for a given nip diameter and loading, and for a specific web strip geometry and material.

In summary, this case study and others have shown that finite element modelling can be used to predict the nip induced tension in a web strip prior to saturation of the nip induced tension due to slippage under the nip. The mechanism of the nip induced tension was discovered via the finite element modelling and comparisons to the classical Hertzian theory. Elastic hysteresis need not be considered in this case since the elongating strain and friction on the lower surface of the web strip dominate the nip induced tension. What remains to be shown is how this knowledge can be applied to the solutions for internal stresses within center wound rolls with an undriven nip roll, which will be discussed next.

INTERNAL STRESS MODELS FOR CENTERWOUND ROLLS

As mentioned in the introduction several models exist which differ mainly in the way which the material parameters are included. The first models, Gutterman [9] and Catlow et al. [10], assumed that a wound roll could be modelled as a linear isotropic material, where the radial modulus was equivalent to the circumferential modulus of elasticity ($E_r = E_\theta$). The next generation of models, Altmann [11] and Yagoda [12], assumed the wound roll could be modelled as a linear anisotropic

material, where E_r is unequal to E_θ although both parameters are assumed to be constants. In reality the radial modulus of a wound roll is a parameter which encompasses both structural and material nonlinearities. Paper, plastic film, and other webs have asperities upon their surfaces and when the web is wound or stacked asperities from one surface contact asperities upon the next surface. Thus upon compression the contact area becomes a function of radial or normal pressure and the measured radial modulus, Er, is a function, typically nonlinear, of radial pressure. Thus the most realistic models of Pfeiffer [13], Hakiel [14], and Willett and Poesch [15] allow for nonlinear anisotropic properties.

Hakiel combined equilibrium, compatibility, and material relationships to yield a second order differential equation in radial pressure:

$$r^2\frac{d^2\sigma_r}{dr^2} + 3r\frac{d\sigma_r}{dr} - \left[\frac{E_\theta}{E_r} - 1\right]\sigma_r = 0 \qquad \{4\}$$

where r denotes a radial location in the wound roll, which requires two boundary conditions for solution. The second order differential equation must be solved several times for the wound roll as the geometry, boundary conditions, and material parameters are continually changing throughout the winding process. Restating equation {4}in a slightly different form:

$$r^2\frac{d^2[\delta\sigma_r]}{dr^2} + 3r\frac{d[\delta\sigma_r]}{dr} - \left[\frac{E_\theta}{E_r} - 1\right][\delta\sigma_r] = 0 \qquad \{5\}$$

Hakiel implemented a finite difference technique to solve equation {5}. Each time the equation is solved, the radial stress distribution obtained must be added to the sum of all the previous radial stress distributions which resulted from previous solutions of the equation or:

$$\sigma_{ri} = \sigma_{ri} + \sum_{j=i+1}^{N} \delta\sigma_{rij} \qquad \{6\}$$

where $\delta\sigma_{rij}$ denotes the radial stress in the ith layer due to the winding on of the jth layer. This procedure is continued until the total N layers have been wound onto the roll. With a known radial stress distribution the tangential stresses can be calculated from the equilibrium expression:

$$r\frac{\partial\sigma_r}{\partial r} + \sigma_r - \sigma_\theta = 0 \qquad \{7\}$$

The boundary conditions for center winding are obtained by considering both the inner and outermost layers of the wound roll. At the inner layer, the radial deformation of the first wound on layer should be equal to the radial deformation of the core. Mathematically this is stated as:

$$u(1) = -\frac{\delta\sigma_r(1)}{E_c} \qquad \{8\}$$

where E_c represents the radial stiffness of the core and u represents the normalized deformation (by dividing by the outside radius of the core) of the first layer. After use of compatibility and material expressions the radial deformation can be eliminated yielding the following relationship:

$$\frac{d\delta\sigma_r}{dr}\Big|_{r=1} = \left[\frac{E_\theta}{E_c} - 1 + \nu\right] \delta\sigma_r \Big|_{r=1} \qquad (9)$$

The second boundary condition involves the outer layer. The circumferential stress, σ_θ, is equivalent to the incoming web tensile stress, T_w, in the outer layer. Treating the outer wrap of the wound roll as a thin wall pressure vessel the radial stress can be related to the circumferential stress via the relationship:

$$\delta\sigma_r \Big|_{r=s} = \{T_w \Big|_{r=s}\} \frac{h}{s} \qquad (10)$$

where h is the web thickness and s is the radial location of the outer wrap.

MODIFICATION OF HAKIEL'S MODEL TO ACCOMMODATE THE NIP

The modification consists of altering the second boundary condition for the center winding model[10]. Referring to Figures 3 and 4 note that for the aluminum web strip that the nip induced tension has reached its saturated value after the nip has rolled five to ten centimeters. The nip induced tensions in the upper five sheets in a stack composed of eight sheets of newsprint is shown in Figure 12. Note that the nip induced tension phenomena resides mainly in the first or uppermost sheet. The result of averaging five such tests, with the exception that a normal pressure was applied to the top of the stack to simulate the radial pressure in a wound roll, is shown in Figure 13. It is clear that the nip induced tension phenomena resides mainly in the first layer. Note that the saturated value of the nip induced tension is approached at approximately 38.1 cm in Figure 12. Tests upon light weight coated papers and upon polypropylene films have shown similar results. Webs are wound upon cores of various diameters but typically not less than 7.62 cm in inside diameter or 8.89 cm in outside diameter. The first wrap would have a circumference of approximately 27.9 cm. Thus for almost the entire winding process which typically consists of thousands of layers the nip induced tension has reached its saturated value. Thus the new boundary condition, which relies principally on the coefficient of friction and the nip loading, may be presented as:

$$\sigma_r \Big|_{r=s} = \left[\{T_w \Big|_{r=s}\} + \frac{\mu N}{h}\right] \frac{h}{s} \qquad (11)$$

where N is the nip loading which may vary through the winding process and μ is the coefficient of friction. After the nip induced tension has saturated, gross slippage of the web has begun to occur on the lower surface of the outer wrap which is in contact with the wrap beneath. Thus the coefficient of friction μ must be the kinetic value of the coefficient of friction.

EXPERIMENTAL VERIFICATION OF THE MODIFIED MODEL

Tests were performed upon light weight coated paper and polypropylene film webs. The web and core properties pertinent to the model input are shown in Table 1. The tests were performed upon a pilot unwind/rewind facility in the Mechanics Laboratory of the Web Handling Research Center[3]. The interlayer radial pressures in the wound roll were measured using Force Sensitive Resistors[4] by Good and Fikes [16]. The radial pressure profiles for the light weight coated web is shown in Figures 14,15, and 16. In each figure the experimental data, the output from Hakiel's model neglecting the nip, and the output from a modified version of Hakiel's model which incorporates the new nip boundary condition is shown. Note in each figure how well the modified model matches the experimental data. A radial pressure profile for a polypropylene web is shown in Figure 17 and again the modified model matches the experimental data nicely.

CONCLUSIONS

The mechanism which is responsible for nip induced tension in wound rolls has been discovered. The mechanism is an elongating machine direction strain which exists beneath the nip roll location on the lower side of the web which is in intimate contact with the wound roll. This elongating strain is due to the compressive Hertzian-like contact stresses which exist through the depth of the web beneath the nip roller. As this elongating strain advances with the moving nip roll, web material attempts to advance in front of the nip and contract in towards the nip in back of the rolling nip. If the web material in back of the nip is constrained a net increase in tension will result due to the nip. The nip induced tension cannot exceed the kinetic coefficient of traction between the outer wrap and the wrap beneath it multiplied by the nip loading, and when summed with the web line tension this is defined as the saturated value of the nip induced tension. Since it was shown that the saturated value of the nip induced tension occurs after short nip rolling distances a new boundary condition was formulated for wound roll stress models in which the tension in the outer wrap was set equal to the sum of the incoming web stress and the saturated value of the nip induced tension. This new boundary condition was incorporated into a model which performs very well when compared to experimental data.

ACKNOWLEDGEMENTS

This publication is a result of research which was funded by the Web Handling Research Center of Oklahoma State University. The authors would like to thank the sponsors of the WHRC for supporting this research. The sponsors include the National Science Foundation, the Noble Foundation, the State of Oklahoma and an industrial consortium of which Beloit Corporation, Polaroid Corporation, Valmet-Appleton Inc., Fife Corporation, Hoescht-Celanese Corporation, 3M Company, Mobil Chemical Company, E.I.Dupont de Nemours & Co.(Inc.), ICI Americas, Kimberly-Clark Corporation, Mead Corporation, Westvaco Corporation, James River Graphics, Eastman Kodak Company and Union Camp

[3] The Web Handling Research Center, An NSF-IUCRC Program, EN 218, Oklahoma State University, Stillwater, OK, 74078.

[4] Force Sensitive Resistors(FSRs^{TM}), Interlink Electronics, P.O.Box 40760, Santa Barbara, CA 93103.

Corporation are members.

REFERENCES

1. Pfeiffer, J.D., 1968, "Mechanics of a Rolling Nip on Paper Webs." TAPPI Journal, Vol. 51, No.8, pp. 77A-85A.
2. Reynolds, O., 1876, "On Rolling Friction." Philisophical Transactions of the Royal Society of London, Vol. 166, pp. 155-174.
3. Reynolds, O., 1874, "On the Efficiency of Belts or Straps as Communicators of Work." Engineer Magazine, p. 396.
4. Tomlinson, G.A., 1929, "A Molecular Theory of Friction." The Philosophical Magazine, Vol. 7, pp. 905-939.
5. Tabor, D., 1955, "The Mechanism of Rolling Friction II. The Elastic Range." Proc. Roy. Soc. A., Vol. 229, pp. 198-220.
6. Hertz, H., 1881, "Uber die Beruhrung fester elastischer Korper." Journal fur die reine und Angewandte Mathematik, Vol. 92, pp. 156-171.
7. Radzimovsky, E.I., 1953, "Stress Distribution and Strength Condition of Two Rolling Cylinders Pressed Together." Univ. Ill. Eng. Expt. Sta., Bulletin 408, pp. 1-40.
8. Bayer, R.G, Shalkey, A.T., and Wayson, A.R., 1969, "Design for Zero Wear." Machine Design, Vol. 41, Pt.1, pp. 142-151.
9. Gutterman, R.P., 1959, "Theoretical and Practical Studies of Magnetic Tape Winding Tensions and of Environmental Roll Stability." US Contract No. DA-18-119-SC-42.
10. Catlow, M.G., and Walls, G.W., 1962, "A Study of Stress Distribution in Pirns." Journal of Textile Institute, Part 3, pp.T410-429.
11. Altmann, H.C., 1968, "Formulas for Computing the Stresses in Center Wound Rolls." TAPPI Journal, Vol. 51, No.4, pp. 176-179.
12. Yagoda, H.P., 1980, "Integral Formulas for Wound Rolls." Mechanics Research Communications, Vol.7, No.2, pp. 103-112.
13. Pfeiffer, J.D., 1966, "Internal Pressures in a Wound Roll of Paper." TAPPI Journal, Vol. 49, No. 8, pp 342-347.
14. Hakiel, Z., 1987, "Nonlinear Model for Wound Roll Stress." TAPPI Journal, Vol. 70, No. 5, pp.113-117.
15. Willett, M.S. and Poesch,W.L., 1988, "Determining the Stress Distributions in Wound Rolls of Magnetic Tape using a Nonlinear Finite Difference Approach." Journal of Applied Mechanics, Vol.55, pp.365-371.
16. Good, J.K., and Fikes, M.W.R., 1991, "Application of Force Sensitive Resistors to Measure Internal Pressures within Wound Rolls." accepted for publication in the June issue of TAPPI Journal.

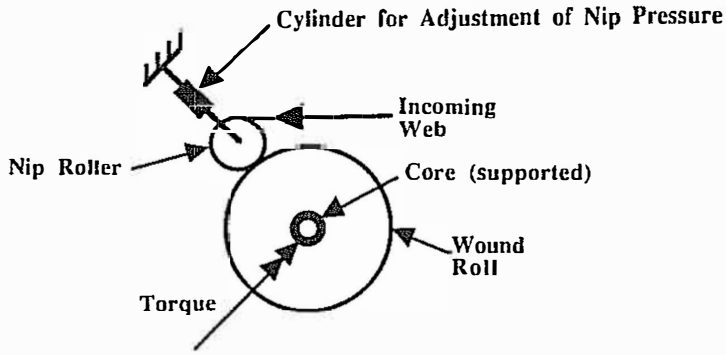

Figure 1. - A Center Winder with an Impinging Nip Roller

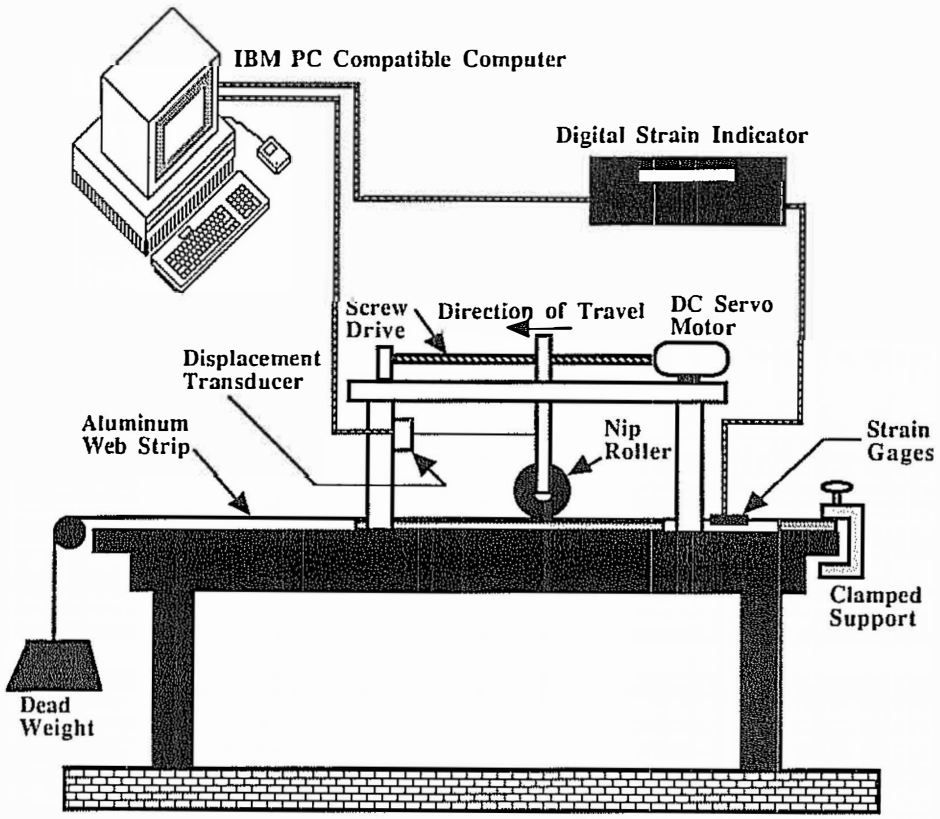

Figure 2. - Experimental Apparatus

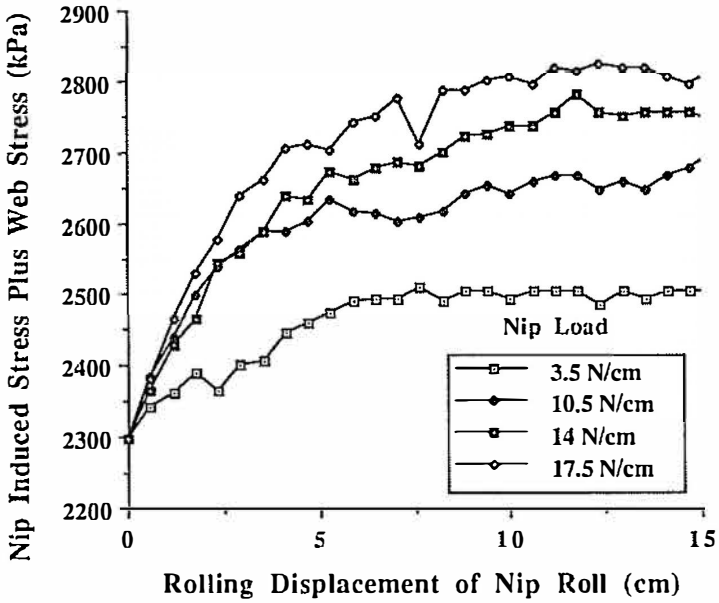

Figure 3. - Nip Induced Stress vs. Rolling Distance for a 5.08 cm Diameter Nip

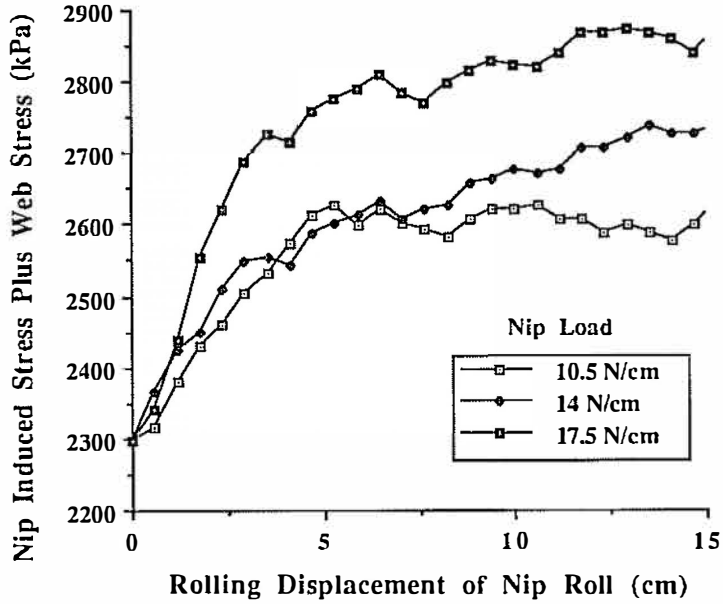

Figure 4. - Nip Induced Stress vs. Rolling Distance for a 10.16 cm Diameter Nip

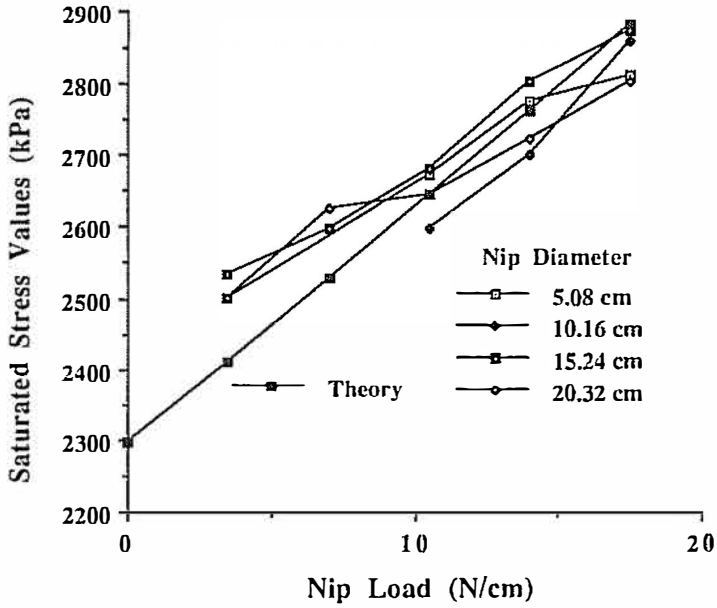

Figure 5. - Saturated Values of the Total Induced Stress

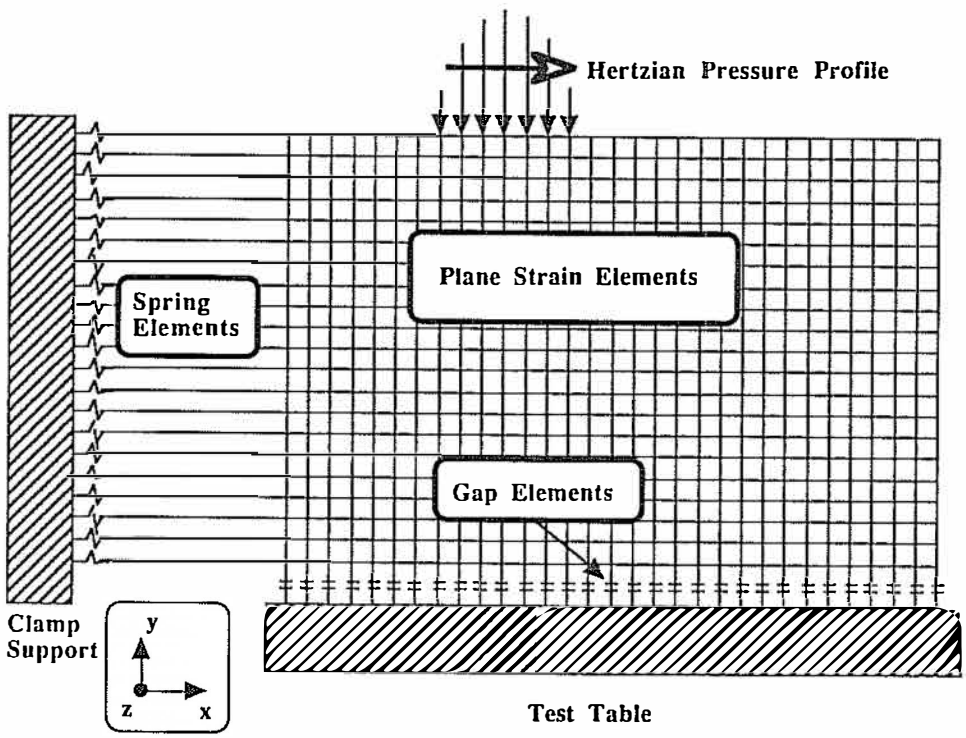

Figure 6. - The Finite Element Model

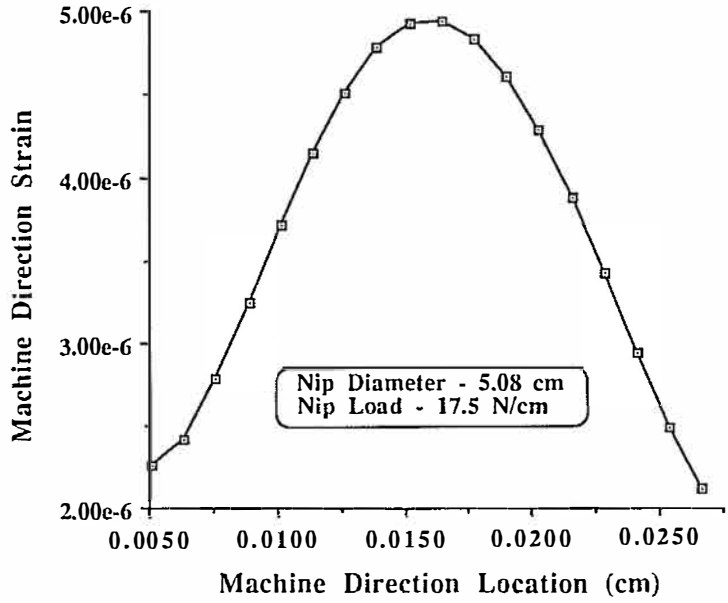

Figure 7. - Strain upon the Lower Surface of the Web Strip Beneath the Nip Roller

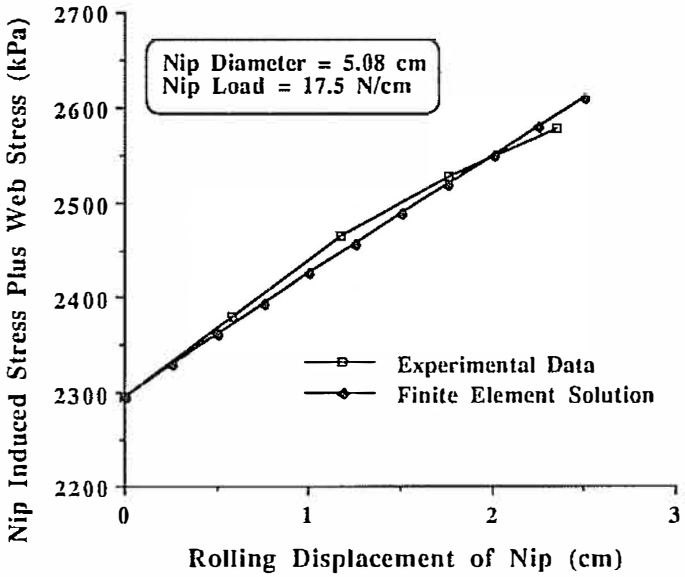

Figure 8. - Comparison of Finite Element Analysis with Experimental Data

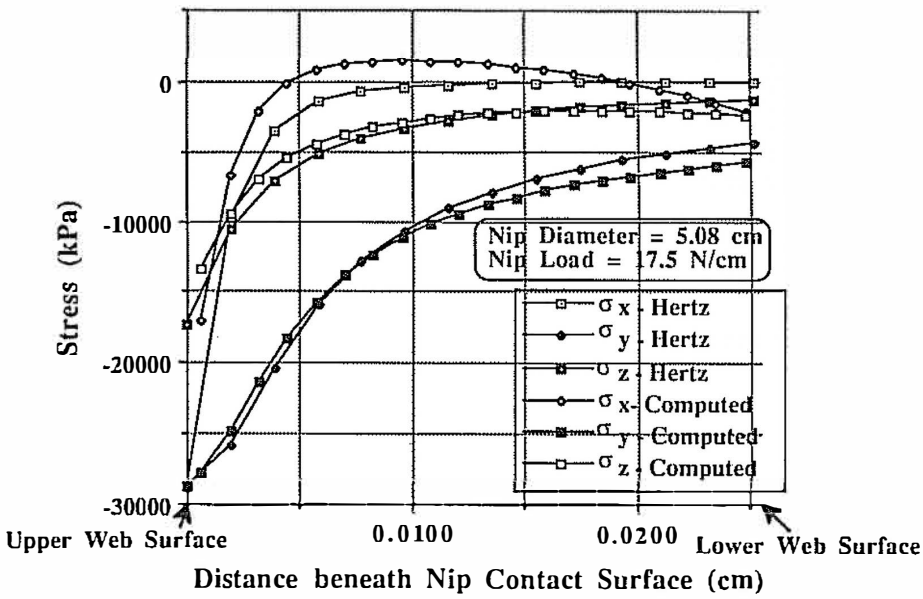

Figure 9. - Hertzian Contact Stresses Compared to Computed Nip Rolling Stresses

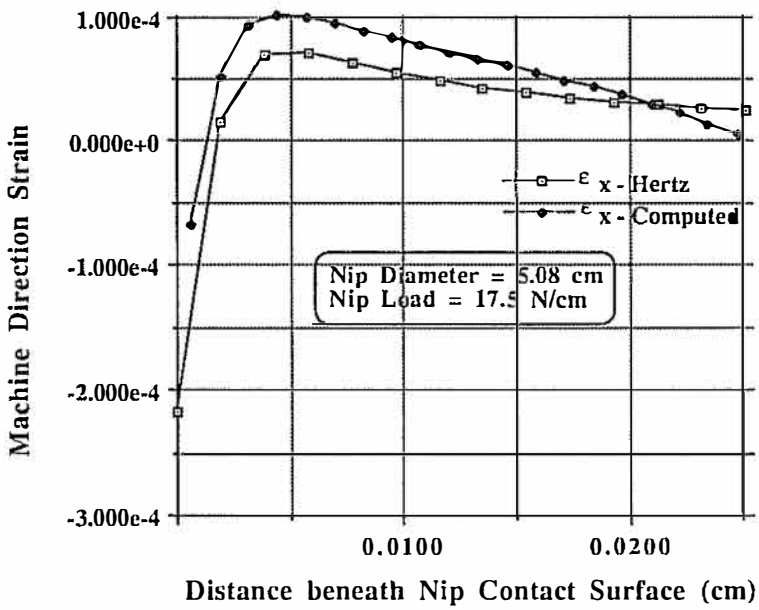

Figure 10. - Hertzian Strain Compared to Computed Nip Rolling Strain

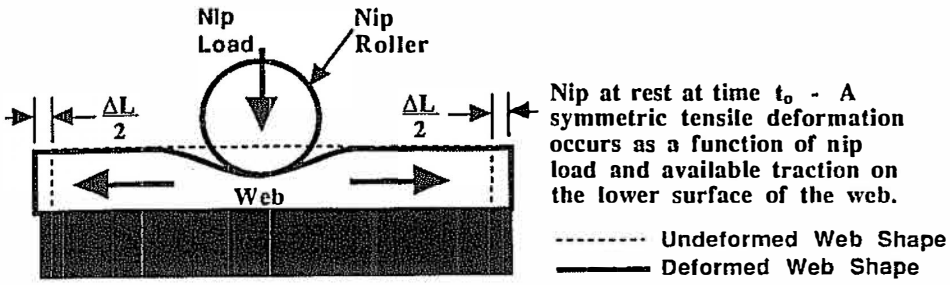

Figure 11a. - Web Deformation due to a Static Nip

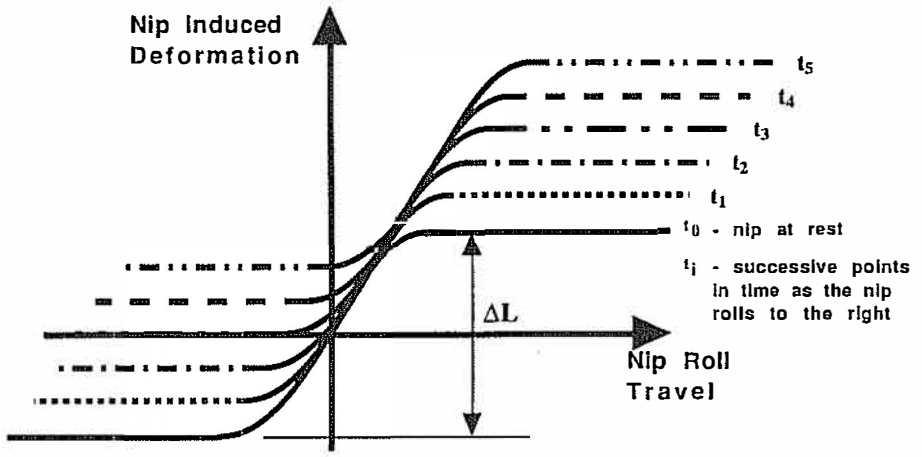

Figure 11b. - Nip Induced Deformations in Stacks or Wound Rolls

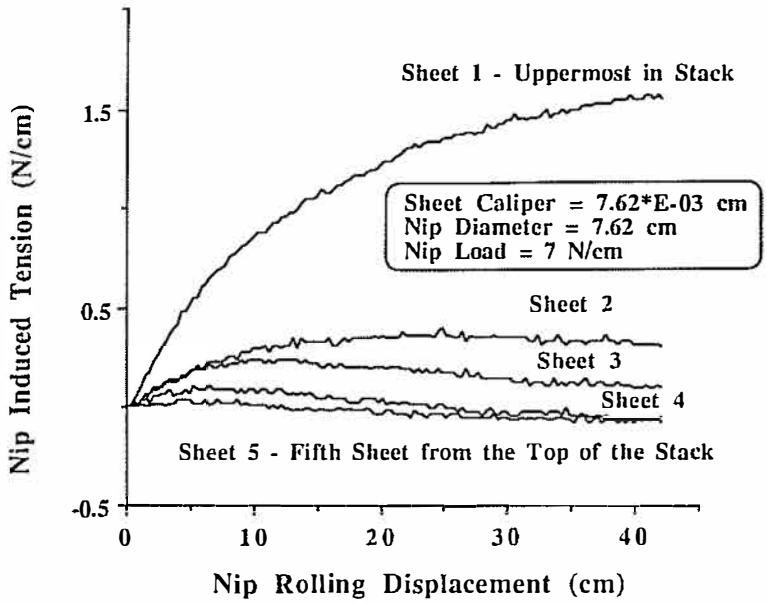

Figure 12. - Nip Induced Tensions in an 8 Sheet Stack of Newsprint

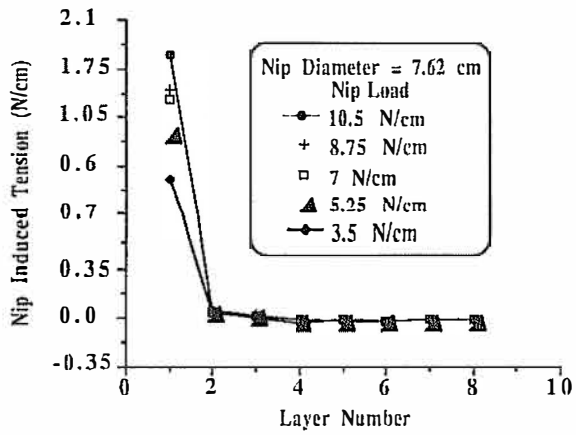

Figure 13. - Saturated Nip Induced Tensions in an Eight Sheet Stack with Simulated Radial Pressure

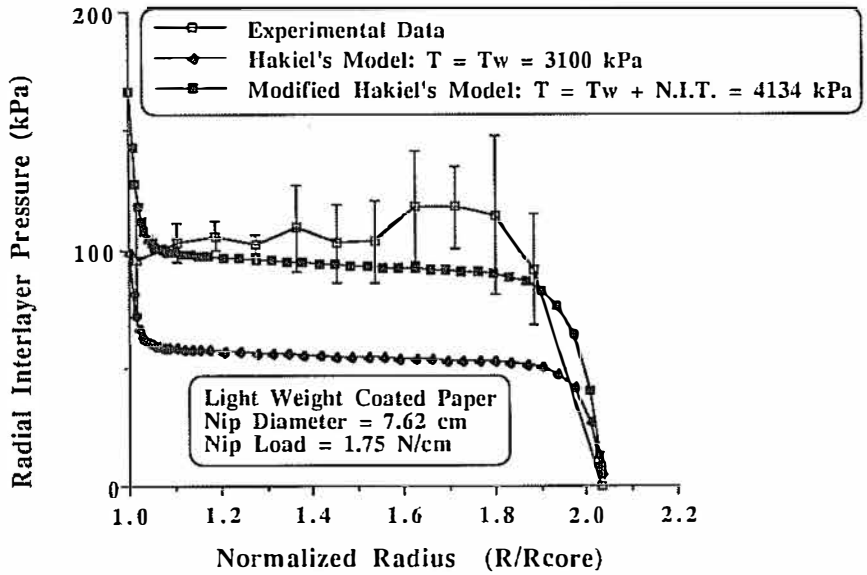

Figure 14. - Comparison of Experimental Results with Hakiel's Modified Model

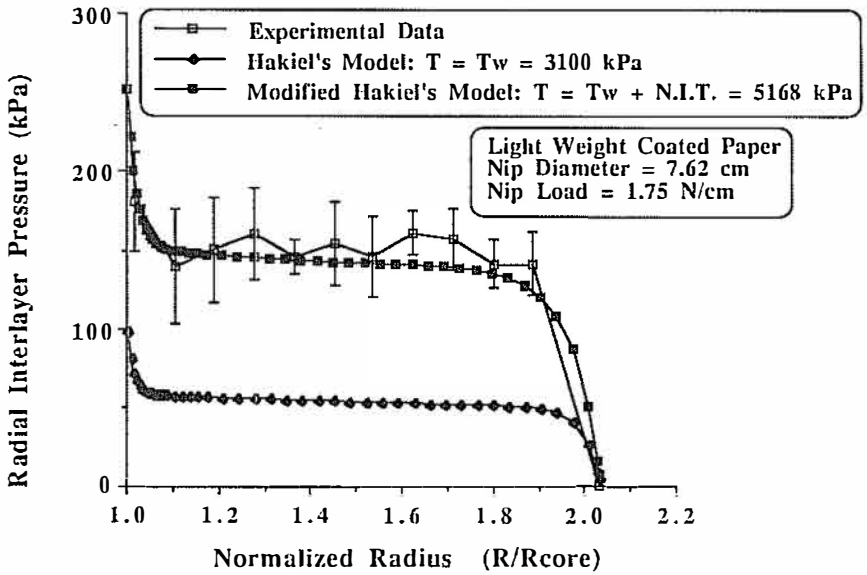

Figure 15. - Comparison of Experimental Results with Hakiel's Modified Model

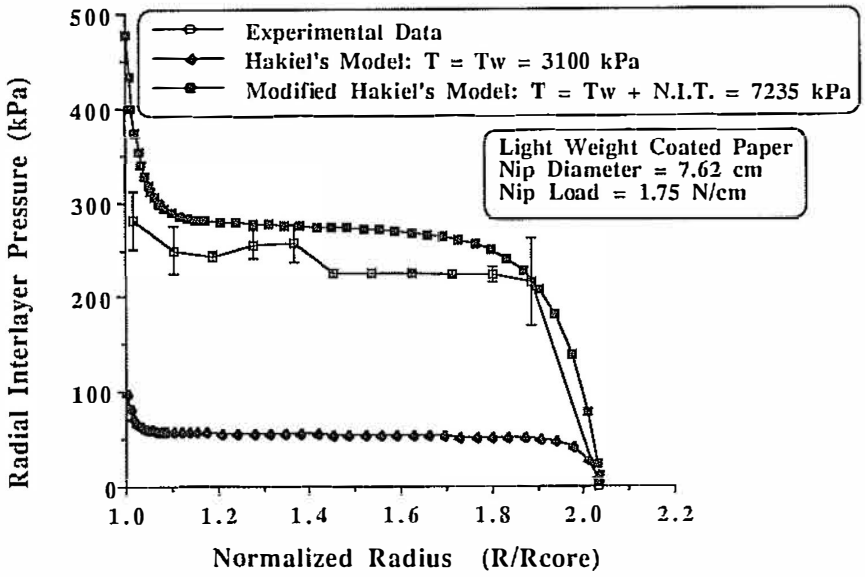

Figure 16. - Comparison of Experimental Results with Hakiel's Modified Model

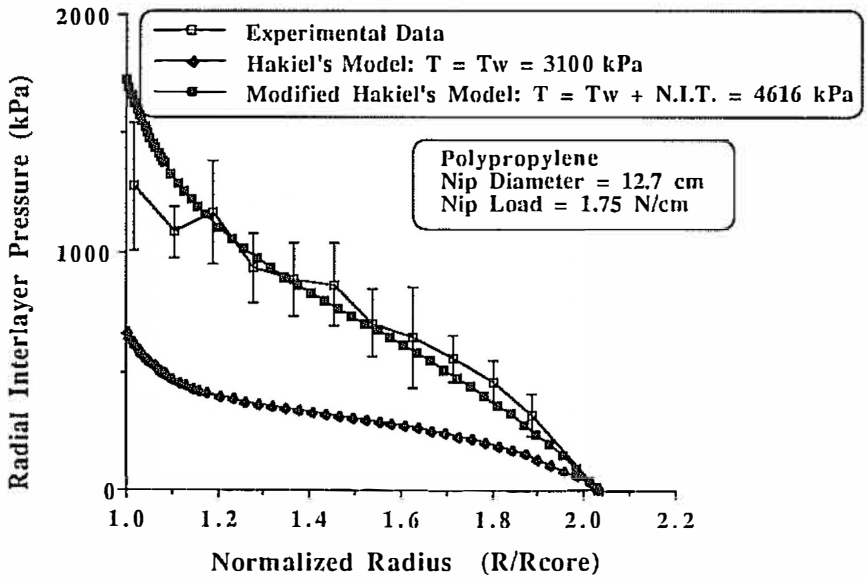

Figure 17. - Comparison of Experimental Results with Hakiel's Modified Model

Table 1
Web Properties and Winding Parameters

	Light Weight Coated Paper	Polypropylene
thickness(cm)	5.08E-03	2.54E-03
width(cm)	15.24	15.24
Poisson's ratio($\nu_{r\theta}$)	0.0[1]	0.0[1]
Er(kPa)	72.8*σ_r	260.0*σ_r
E_θ(GPa)	8.268	3.101
coefficient of traction	0.30[2]	0.22[2]
core i.d.(cm)	7.71	7.71
core o.d.(cm)	8.75	8.75
core stiffness steel(GPa)	27.1	27.1
final roll diameter(cm)	17.78	17.78

1. Poisson's ratio as a stack property was assumed to be zero as assumed by
Hakiel[15].

2. Kinetic values of the coefficient of friction.

STRESSES WITHIN ROLLS WOUND IN THE PRESENCE OF A NIP ROLLER

J.K. Good

Are there significant changes in the nip induced tension when using an aluminum lay-on roll where the primary deformation occurs in the product roll vs. a low durometer elastomeric roll where deformation can occur in the lay-on roll itself?

Al Gladowski, Parkinson Mfg.

Yes there are differences and by the techniques that I've just shown you. you can investigate those effects. Remember I employed a finite element model. The half-width of the Hertzian contact parabolic pressure distribution is controlled by the elastic moduli of what we are resting upon and by the elastic moduli of the nip that's rolling upon it. My point is that if you want to investigate the effect of elastomeric coverings on rolls this technique will allow you to do it. What will happen is that I would expect for the same nip diameters and nip pressures that this distribution would spread out. There would be a change in the nip induced strains in the layer beneath the nip, and the rate would change at which the nip induced tension would increase. I don't see any reason why the saturated value of the nip induced tension should change and give you a different value of the winding or wound in stresses in the center-wound roll.

Could this theory be adapted to a two drum or a single drum winder?
Dave McDonald, Pulp and Paper Research Institute of Canada

I see no reason why it couldn't be. Why not at least in the finite element model? There is nothing to say you can't have two hertzian pressure profiles moving across this strip if you want to see the rate at which the nip induced tension is increased. There are certainly some different things that one has to be able to handle with the two drum winder especially when you're running in the differential torque arrangement. If you've got slippage or the web breaking loose from the outside of the wound roll certainly the stress in the outside layer can be a function more of that differential torque then it would be due to the nip effects.

Is there an equally simple boundary condition for driven lay-on rollers that can be used with the center winding models?
Zig Hakiel, Kodak

I'm trying to figure that out right now. I'm taking the approach where I study one boundary condition at a time.

It is my observation that the friction limit is the most tension you can achieve, but that if you were to use nip forces as high as 70N/cm, which I used in the WIT-WOT paper, you would find both a curved response and a nip roller diameter dependence.
Dave Pfeiffer, McGill University

The analyses in this study are totally in the elastic realm. Various combinations of nip loads and diameters could certainly result in strains in the wound on layer which are beyond the elastic strain domain of a particular web. I believe what you say is true but the intent of this study was to discern why the nip induces tension in the elastic domain of the web material. A nonlinear finite element program has to be employed in this study to accomodate the slippage beneath the web. Certainly material nonlinearities could be incorporated in to these analyses as well with the same code.